Frontiers in high-pressure physics research

R. Chidambaram and Surinder M. Sharma

Studies of materials and the discovery of various novel and unexpected phenomena under high pressures have contributed immensely to our understanding of the behaviour of matter. The variety of phase transitions observed display systematic patterns, giving insights into the underlying physics. There are many similarities and significant differences in the phenomena observed under static and dynamic (shock) pressure loading. This article presents experimental and theoretical developments in this fascinating field.

Research at high pressures has truly developed into an interdisciplinary area which has important implications for and applications in the areas of physics, chemistry, materials science, planetary sciences, biology, engineering and technology. Apart from the discovery of various novel and unexpected phenomena, high-pressure research has provided new insights into the behaviour of matter. These developments have also inspired significant theoretical developments.

One of the most important outputs of high-pressure experiments is the pressure–volume–temperature relationship of materials termed the equation of state (EOS). Its utility for any meaningful interpretation of physical and chemical phenomena under pressure cannot be overstated. For example, questions like how the criticality factor for a fissionable mass varies with compression cannot be answered otherwise. This is also a vital input to evaluate rock-mechanics effects of underground peaceful nuclear explosions[1,2]. For the physics of condensed matter, it provides a stringent test for interatomic potentials and for the theories of cohesion and of a variety of phase transitions (like solid–liquid, insulator-to-metal, valence transitions, etc). In geophysics, this helps towards an understanding of the inner structure of the earth, and in astrophysics to unravel the evolution of stellar bodies like white dwarfs, neutron stars and black holes. In recent years, considerable theoretical developments have also taken place in the field of high-pressure research and we are beginning to understand well the underlying physics[3,4].

Pressure-induced phase transitions are a very general phenomenon and the study of these continues to be the most active area of high-pressure research. Also this is intimately connected with the materials synthesis aspect. The generation of various superhard materials including synthetic and sintered diamonds has come about from this research. For example, formation of synthetic diamonds and cubic boron nitride is due to transformations under high pressure to phases which are metastable under ambient conditions[5,6]. Aside from applications, the phenomena related to phase transitions are basically very interesting. Recent discoveries of amorphization of crystalline materials under pressure is an example of this kind[7,8]. The general principle of corresponding states[9], which implies similar phase diagrams for a column of elements in the periodic table, seems to work only at low pressures. At high pressures, where details of electronic structure become important, this principle breaks down even for rare gas solids and is replaced by the trends imposed by $s \rightarrow d$ transitions (see section on transition metals). For example, at a pressure of 1 bar (or one atmosphere) most of the metallic elements have close-packed structures while non-metallic elements of the upper right-hand corner of the periodic table have open structures due to covalent bonding. The increase in pressure destabilizes covalent bonding by increased electron delocalization and the open structures evolve towards dense packing. However for metallic elements, including rare earths and actinides, $s \rightarrow d$ (or f) transfer stabilizes structures with directional bonding, such as α–U. There is some evidence that at still higher pressures ($\gg$ 100 GPa) where $s \rightarrow d$ transfer is complete, the structures will revert back to dense packing[10]. (1 GPA = 10 kilobar = 10^4 bar, where one bar = 10^5 Nm^{-2} = 0.9869 atm = 1.0197 kg cm^{-2}. A megabar = 100 GPa.)

Interspersed with the structural transformations are electronic transitions which either show up[11] in EOS or do not depending upon the nature of electronic changes[12,13]. The exciting problem of metallization of hydrogen under pressure seems getting close to be settled but still eludes a definite answer. In principle, one expects hydrogen to metallize before dissociation[14], like iodine[15], and the additional phase transition to the orientationally ordered phase[16] lowers the pressure of metallization[17]. The infrared reflectance measurements[4]

This article is based on the IISc Golden Jubilee Memorial Lecture 1991 delivered by R. Chidambaram on 15 March 1991 at the Indian Institute of Science, Bangalore

The authors are in Bhabha Atomic Research Centre, Trombay, Bombay 400 085.

show a characteristic free electron behaviour (represented by Drude-model) giving the metallization pressure of 149 (±10) GPa, consistent with a recent first principles quasiparticle calculation of indirect band overlap[17] in the orientationally ordered phase. However, the reflectance measurements are not consistent with the absorption measurements[18] and the former may have alternative interpretation in terms of hydrogen reduction of ruby at high pressures[19]. We suggest that an X-ray diffraction study of hydrogen and ruby mixture at high pressure (> 150 GPa) should be able to identify the Al, if, indeed, the hydrogen reduction of ruby takes place. CsI and Xe which are insulators at ambient and low pressures have been shown to become metallic at 110 GPa and 130–150 GPa respectively[20,21]. It is worth noting that a first-principle quasiparticle calculation (similar to that for hydrogen) of this transition in Xe predicts the transition to be 128 GPa, in very good agreement with the reported observations[22].

There have been some high-pressure investigations of organic materials[23,24] as well as of materials of significance to biologists[25,26]. Organic materials too show phase transitions resulting in denser packing but such studies have been restricted to low pressures and detailed systematics are not known.

In a nutshell, the field of high-pressure physics continues to be an area of intense activity throwing up many challenging problems worth deeper study.

The highest pressures achieved

In Table 1 we have summarized the present experimental situation for all kinds of experimental systems designed to generate high pressures. However, the stress/strain state accompanying the highest pressures is often not well characterized. In the diamond cells the possibility of high non-hydrostatic stresses may complicate the situation. And for dynamic pressures the existence of a steady state may be debatable. Notwithstanding this, by careful experimentation and appropriate modelling, it is possible to obtain a very considerable amount of valuable information.

For comparison let us examine the pressures to which geological materials are subjected to in nature. In the centre of the earth the pressure is about 360 GPa and at a depth of about 2900 km—the boundary between the mantle and the core—it is about 150–200 GPa. Typical pressures at the greatest depths in oceans are about 0.1 GPa. So already even in the static experiments, pressures greater than those at the centre of the Earth can be achieved. But when compared with the giant planets like Jupiter and Saturn, at the centres of which the pressures are about 4500 GPa and 1000 GPa respectively, the pressures reached in static experiments are still far too low. However, useful insights could already be obtained. For example, hydrogen is thought to be the most dominant material in both Jupiter and

Table 1. The highest pressures achieved through various experimental techniques (adapted from Godwal *et al.*[3])

Method	Type of measurement	Maximum pressure (GPa) achieved	Typical V/V_0 achieved†	% Error in pressure estimation (%)
Static methods				
Piston cylinder	Isotherm	4.5[a]	0.95	3
X-ray diffraction	Isotherm	416[b]	0.4	10
Shock waves				
Chemical explosive	Hugoniot (principal and reflected)	1000[c]	0.5	2
Gas-gun	Hugoniot (principal and reflected)	500[d]	0.5	1
Laser	Hugoniot (principal and reflected)	3500[e]	0.3	20–30
Underground nuclear explosive	Hugoniot (principal and reflected)	500,000[f]	0.3	2–5
Electric gun	Hugoniot (principal and reflected)	1000–5000[g]	–	–
Rail gun	Hugoniot (principal and reflected)	1000–10,000[h]	–	–
Magnetic compression	Isentrope	500[i]	0.25	–

[a]Vaidya and Kennedy[134]; [b]Ruoff *et al*[135], [c]See Van Thiel[136] for compilation of these data, [d]Mitchell and Nellis[137], [e]Trainor *et al*[138]; [f]Vladimirov *et al*[139]; [g]Weingart *et al.*[140], projected values; [h]Hawke and Scudder[14], projected values; [i]Hawke *et al*[142]

†Depends on the material.

Saturn and hence we can say that, for the most part, hydrogen should exist in a metallic form in these planets.

Phenomenology of Pokhran PNE experiment

India's first and only peaceful nuclear explosion experiment was carried out on 18 May 1974 in the Rajasthan desert at a place near Pokhran. The objective of the experiment[1] was to study the explosion phenomenology, fracturing effects in rocks, ground motion, containment of radioactivity, etc. In the Pokhran experiment, a plutonium device of yield 12 kt equivalent of TNT, was emplaced in a shale medium, at a depth of 107 m in a chamber at the end of an L-shaped hole. Upon detonation, the ground surface above the emplacement point rose with a velocity of 25–30 m sec^{-1} to form a dome 170 m in diameter and 34 m in height. There was no venting of radioactivity in the experiment. The resultant apparent crater, measured with respect to the preshot ground surface, had an average radius of 47 m and a depth of 10 m.

The phenomenology of this experiment was explained by Chidambaram *et al.*[2] using computer modelling with a one-dimensional spherical symmetric rock mechanics computer code. On a sudden release of explosive energy of a nuclear device, various physico-mechanical processes are set up in the geological medium, like vaporization, melting, crushing, fracture and motion of the surrounding rock. The reflection of stress waves at the free ground surface transfers additional kinetic energy to the rock medium. The final crater dimensions depend upon the total kinetic energy transferred to the region above the explosion-produced cavity

Most of the energy of the Pokhran device—as in any other nuclear explosive—was released in less than a microsecond. Our calculations show that this resulted in 640 tons of rock, extending up to 4.1 m from shot point, being vaporized. About 2000 tons of rock, extending up to a radial distance 6.2 m, was shock-melted. At the vapour-liquid interface, the pressure is expected to be about 160 GPa. Computed wave propagation and cavity growth are shown in Figure 1. The final cavity radius in the horizontal direction is calculated to be about 28–29 m compared to the post-shot measured value of 30 m. For more details the reader may refer elsewhere[1,2].

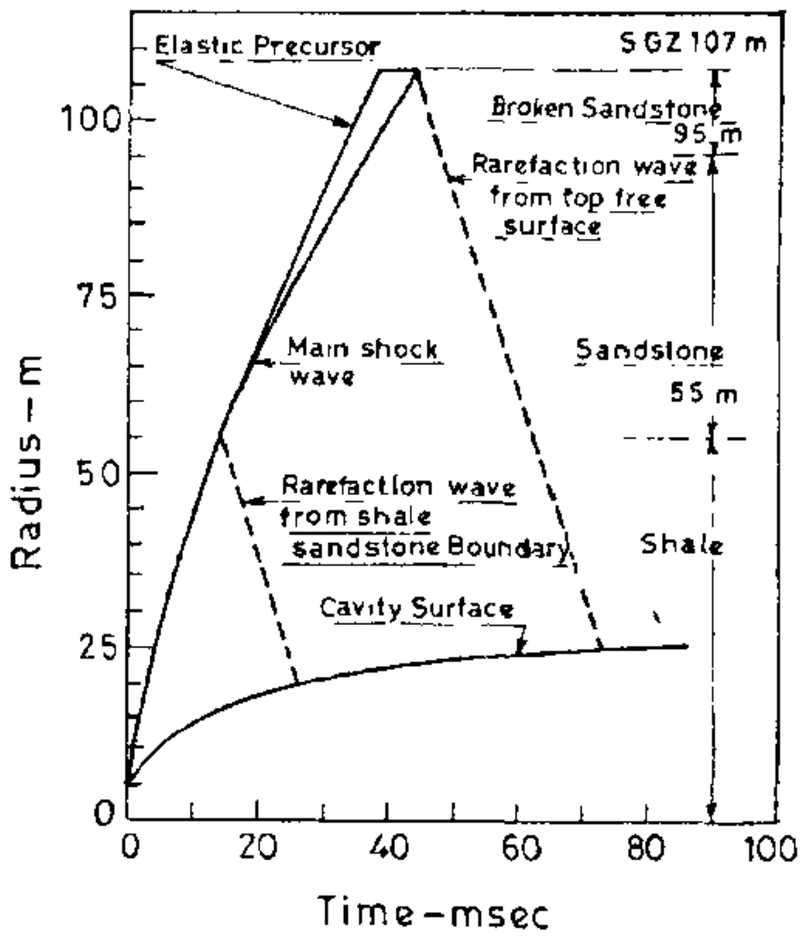

Figure 1. Computed wave propagation and cavity growth in vertical direction for the Pokhran experiment. [Ref. 2]

Mechanism of phase transformations

Over more than a decade, our laboratory at Trombay has been engaged in the study of phase transformations in materials under static high pressures. Various techniques have been set-up and used in these experiments. These include four-probe resistance measurements, WC anvils with Be gaskets for angle dispersive X-ray diffraction[27] and the diamond anvil cell (DAC)-based full Bragg cone, energy dispersive X-ray diffraction system (EDXRD) along with a ruby fluorescence spectrometer[28] to measure the pressure. Since 1987, most of our studies have been carried out in the DAC-based EDXRD system (see inset in cover picture). We use the white X-ray beam from a rotating anode X-ray generator (GX-20, Marconi Avionics) with a total power loading of 2.2 kW at the focal spot of 0.2×2 mm^2. A collimator collimates the beam to about 100 μm, about 5 mm away from the sample mounted in our DAC. The diamond cell, based on the design of Hubert *et al.*[29], has been fabricated indigenously in our workshop. We use diamonds of 0.3 carat with a culet diameter of 0.5 mm. The powdered sample is contained in a hardened Inconel or steel gasket with a central hole of about 150 μm. A 16:3:1 mixture of methanol, ethanol and water is the typical pressure-transmitting fluid used. The diffracted beam is collected over the full Bragg cone by a conical slit of $4\theta = 26^\circ$ (or 20), giving the diffraction pattern for d spacings between 1 and 5 Å. The diffracted beam is energy-analysed using a large area (36-mm dia) HPGe detector (ORTEC) and our indigenous 8085 microprocessor-based MCA. More details are given elsewhere[30]. Now a new diamond cell, similar to the Mao and Bell type, has been fabricated in our workshop and this DAC-based angle-dispersive system using the film method is being commissioned by our colleagues, Vijayakumar, Meenakshi and Godwal. We now discuss studies carried out in our laboratory at Trombay, where a useful interaction of experiments and theory has helped us discover the path of many transformations we have studied.

In the group IIb, most elements exist in the hcp phase under ambient conditions while Hg crystallizes in

the body-centred tetragonal (bct) phase. Hg_xCd_{1-x} alloys stabilize in the bct structure if x is greater than 0.25 and in the hcp phase for lower values of x. From the generalized phase diagram, calculated by Hafner and Heine[31], it can be argued that under pressure the bct phase of Hg should transform to the hcp phase. Alloying with Cd essentially lowers the pressure of transition. We studied two alloys ($x=0.35$ and 0.5) which transformed to the hcp phase at 2 GPa and 6.4 GPa respectively[32,33]. A closer look at the two structures shows that these are related by correlated atomic motions characteristic of a $TA_1(110)\langle 1\bar{1}0\rangle$ zone boundary phonon mode. In addition, one requires the existence of a uniform strain to change the angle in the hexagon ($=124.5°$ in $Cd_{0.65}Hg_{0.35}$) to 120°. These structures could evolve from each other within the description of an orthorhombic supercell as shown in Figure 2.

In view of a possible coupling between the shuffle and a uniform strain, a detailed frozen-phonon calculation was carried out[33]. Using Andersen's force theorem and the band structural contribution from a LMTO calculation, the phonon frequencies of the zone boundary TA_1 mode were computed. The calculation showed a strong coupling of the degree of softening with an increase in the c/a ratio. This coupling permits us to use two coupled strains in the framework of Landau theory[34] to explain the observed phase transition. The experimental study did show the increase in c/a with pressure as required by theory. Recently, even in pure Hg, the expected bct to hcp transformation has been observed[35].

This study brought into focus the well-known martensitic transformation at low temperatures from the ambient bcc phase of Na. The low-temperature phase of Na has been variously indexed as hcp[36], 9R with stacking faults[37] or the latter with various additional higher order polytypes[38]. Figure 2 shows that the path of this transformation should be similar to that observed in Hg and CdHg alloys.

Sankaran, Sharma and Sikka have carried out total energy calculations using LMTO as a function of three variables: (i) angle θ (shown as 109.47° in Figure 2); (ii) the required atomic displacement (shown by arrows in Figure 2), and (iii) the d spacing of (110) planes. When the total energy is plotted in the hyperspace of these variables, it shows the existence of essentially a barrierless path from bcc to hcp. This makes a continuum of intermediate orthorhombic structures accessible. So the structure could be trapped anywhere in this path depending upon microstructural stresses and strains. This suggests an inherent irreproducibility of the structure, in conformation with experimentally observed diffraction patterns. The increased broadening of the diffraction peaks can then be explained as being due to an ensemble average over intermediate structures. A model calculation shows the lack of any diffraction peaks in the region 2.2 to 2.8 Å of d spacing, which is consistent with the observed results. So we proposed[39] that the low-temperature phase of Na is the 'ensemble of intermediate distorted orthorhombic structures' of space group Cmcm. The situation is analogous to that of CsI which undergoes a phase transition[40] at about 100 GPa which eventually evolves to a hcp-like phase around 300 GPa. The structure here is again distorted-orthorhombic and evolves continuously from B 2 (<100 GPa) to hcp (>300 GPa).

Another example of this kind is Si, which shows a large number of phase transitions[41] under pressure. Of particular interest here is the phase transformation from β-Sn to primitive hexagonal occurring at about 16 GPa. The structural relation between these two phases can be understood in terms of the softening of $\frac{1}{2}(101)_{ph}$ phonon mode[42]. Our lattice dynamical calculations employing pseudopotentials showed the softening of this mode as required. A recent neutron scattering study on Sn, stabilized in the primitive hexagonal phase by alloying, confirmed[43] that the above-mentioned mode indeed is soft as predicted by us.

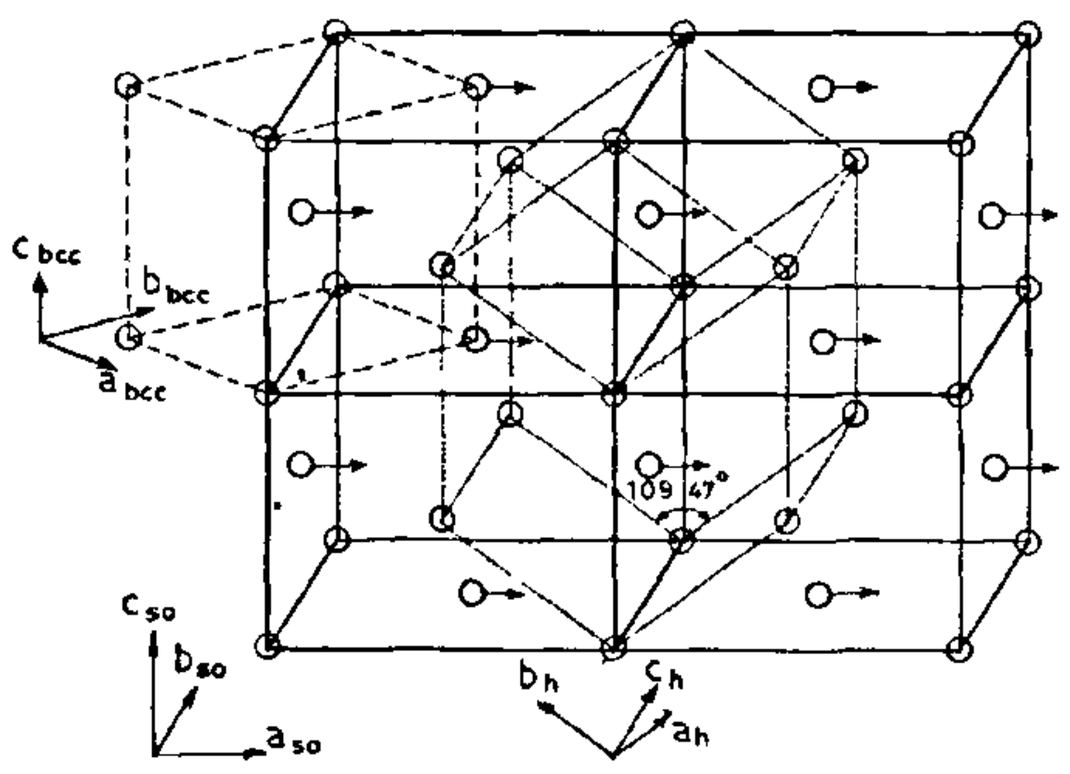

Figure 2. The path of transformation from a bcc phase to hcp phase via distorted orthorhombic cell as in Na [ref. 39]. For bct to hcp phase transformation observed in Hg_xCd_{1-x} alloys, the initial cell is bct with the angle $\theta = 124.5°$ instead of 109 47°, shown in the figure. This can be generated by appropriate choice of a, b, c of simple orthorhombic cell. [Refs. 32, 33].

Amorphization under pressure

$LiKSO_4$ has a stuffed tridymite structure with three-dimensional networks built of six-membered rings of vertex-linked LiO_4 and SO_4 tetrahedra with K in large open interstices. It is well known that coordination polyhedra joined at vertices have several configurations, with different relative orientations of polyhedra but with roughly the same energy[44,45]. This, coupled with the possibility of different polyhedra having different

compressibilities, explains the abundance of phase transitions caused by polyhedra tilting. After extensive studies of this material as a function of temperature at Trombay[46-48] we undertook the study of phase transitions under pressure.

The *diffraction* pattern of the compound under increasing pressure is shown in Figure 3 (Figure 3,*a* without any pressure calibrant and Figure 3,*b* with Au as pressure marker). At higher pressures the diffraction pattern develops superlattice lines (shown by arrows). But the resolution of our EDXRD system did not permit the identification of the new phase. It was difficult to differentiate between the incommensurate phase (β) or the lock-in phase (γ), suggested by an earlier Raman study[49]. At still higher pressures, a broad glass-like background increased with a simultaneous decrease in the intensity of Bragg lines. The diffraction pattern completely disappeared at about 13 GPa. The crystalline form re-emerges on release of pressure after about 72 h. Figure 3,*b* shows that the diffraction pattern of Au continues to exist, ruling out any experimental error. So $LiKSO_4$ becomes amorphous[7] at 13 GPa and this has been confirmed by a recent Raman scattering study[50] under pressure.

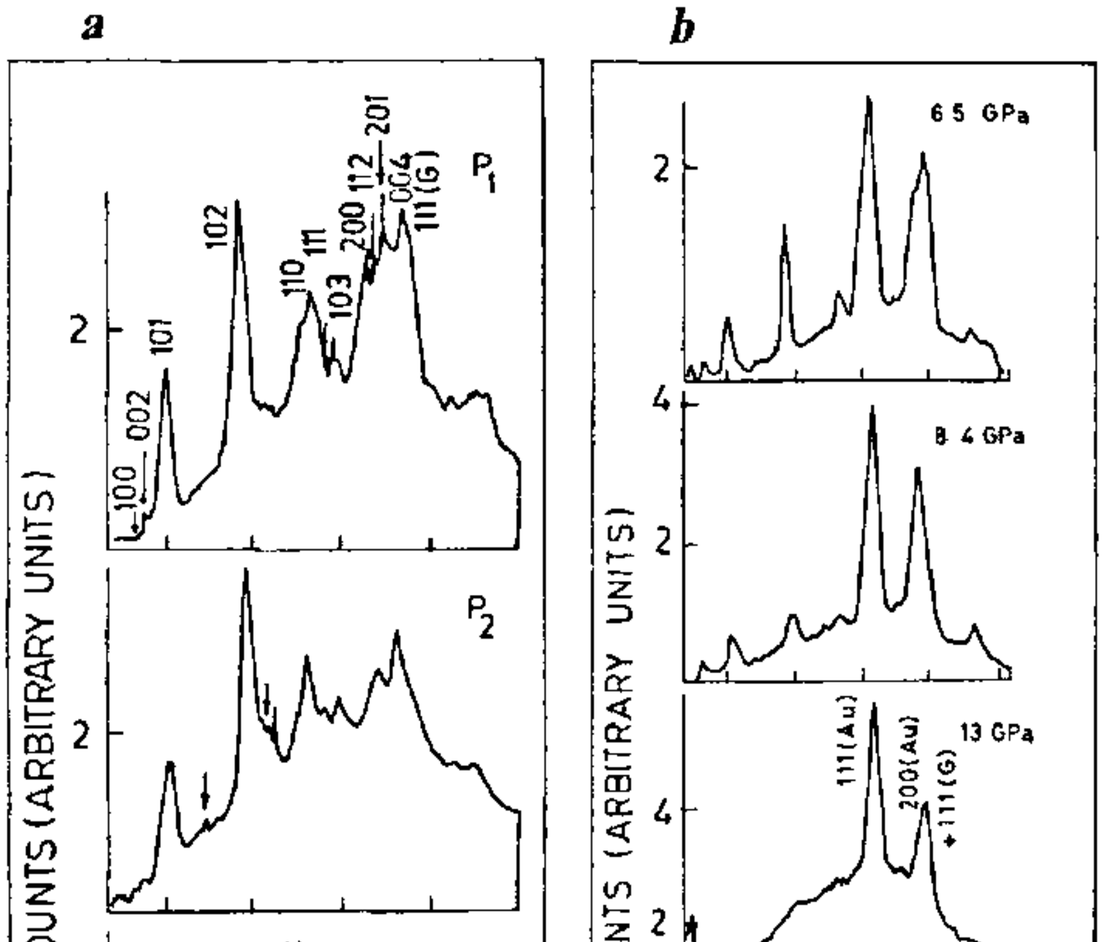

Figure 3. *a*, Diffraction patterns of $LiKSO_4$ recorded at different pressures ($P_1 < P_2 < P_3$) without any pressure marker, G denotes gasket diffraction peaks. [Ref. 7]. *b*, Diffraction pattern of $LiKSO_4$ with *in situ* Au marker at 6.5, 8.4 and 13 GPa and after release of pressure (Ref. 7).

More or less at the same time, quartz and the cocsite phase of SiO_2 were shown to amorphize under pressure by Hemley *et al.*[51] They suggested that amorphization in quartz may be related to the reduction of intertetrahedral Si–O–Si angle from about 145° towards 120°. This prompted us to study $AlPO_4$, a compound isostructural to quartz[52]. In this compound Al–O–P angle is about 142° at ambient conditions[53]. The compression leads to an increase in *c/a* implying a reduction of Al–O–P angle. At 12 GPa, $AlPO_4$ turned amorphous[8]. This has been confirmed by an independent study by Jeanloz *et al.*[54] By now many materials like ice, SnI_4, TCNE, SiO_2, $CaAl_2Si_2O_8$, $Ca(OH)_2$, Fe_2SiO_4, etc. have been amorphized under pressure[8]. A recent Raman scattering study[55] on the organic material resorcinol shows a complete vanishing of lattice modes at 5 GPa, which is very similar to what has been observed[50] for $LiKSO_4$. This suggests the amorphization of resorcinol at about 5 GPa. It is known that organic materials undergo polymerization (a chemical transformation) at still higher pressures (about 30 GPa for benzene[56]). So the loss of lattice modes at considerably lower pressures (5 GPa) is unlikely to be due to polymerization. Instead, a probable cause of amorphization may be the breakdown of hydrogen bonding which is central to the stability of the α and β phases of resorcinol[23]. If this is the case it would show up in the measurements of H–O stretching mode. This mode is expected to soften somewhat on initial pressurization and around 5 GPa it should jump back to a higher value, symptomatic of breakdown of hydrogen bonding. The experiments are in progress to test this. Because the polymerization is expected at considerably higher pressures, one can expect the emergence of another crystalline phase before polymerization. A recent molecular dynamical study of SiO_2 and $LiKSO_4$ at Trombay shows that the amorphous phase in these structures results from the frustration of the tendency of crystalline units to increase atomic coordination under pressure[57,58].

Transition metals

Unlike other elements the occupancy of *d* and *f* bands plays a vital role in stabilizing a structure in the transition metals, the rare earths and the actinide series. For 3*d* transition metals it was shown by Pettifor[59] that the structure is essentially decided by Nd: the number of electrons in the *d* bands. Subsequent work of Williams[60] and a simple calculation based on canonical bands and *d* occupancy by Skriver[61] firmly established the significance of *d* bands in the transition metal series. From the viewpoint of high pressures it is important to realize that various bands move and broaden under pressure resulting in band crossing and consequent electron transfer[62]—often from *s(p)* bands to *d(f)* bands.

Due to this, even simple metals like Mg and Cs behave like transition metals at high pressures. For example in Mg, hcp to bcc phase transition at about 50 GPa is due to $s \rightarrow d$ transfer[63]. In general $s \rightarrow d$ transfer could lead to significant softening of EOS or give rise to phonon anomalies and consequent phase transformations[62] as in Cs. As pointed out in the introduction above, $s \rightarrow d$ transfer under pressure is central to the understanding of structural changes under pressure right across the periodic table; its signatures are visible in transition metal series even at quite low pressures.

In the transition metal series, our group has carried out extensive studies, particularly on Ti, Zr and Hf. This work started with studies of the ω phase in Ti and Zr in the seventies. Ti transforms from hcp (α) to the simple hexagonal (ω) phase in the pressure range[64] 2.9–7.5 GPa while, for Zr, transformation to the ω phase occurs[64] between 2.1 and 6.0 GPa. In both the materials the ω phase is metastable and is retained on release of pressure. Under appropriate thermodynamic conditions, materials could be completely transformed to the ω phase[65]. Detailed band structure calculations, XPS and positron annihilation studies were carried out on the α and ω phases[65,66]. The stability of the ω phase was shown to be related to $s \rightarrow d$ transfer[65,67]. The issue of how the α phase transforms to the ω phase has also been settled unambiguously. From the orientation relations between the α and ω phases in pressure-treated Ti and Zr foils, Usikov and Zilbershtein[68] had suggested that the α phase goes to the ω phase via an unstable β phase. The evidence of this intermediate β phase was found by Vohra *et al.*[69–71] in dilute Ti–V alloys. Selected area electron diffraction patterns obtained from pressure-treated Ti-10% V showed all the three phases while the sample had only the α phase to begin with. The observation of the four expected variants in the ω phase confirms that β occurs as an intermediate phase. The validity of this conclusion for pure Zr was shown by the study of orientation relations between α and ω phases by texture studies using the neutron diffraction method by Gupta *et al.*[72] The rocking curve of the fully transformed ω-Zr is shown in Figure 4. While Figure 4,*a* shows that either or both of the possible variants may be present, the absence of the second order $(20\bar{2}2)_\omega$ reflection in Figure 4,*b* confirms the coexistence of both the variants. More details have been presented in an extensive review article by Sikka *et al.*[64]

The equation of state and the structural stability of Ti, Zr and Hf were also calculated using the LMTO band structural method[67,73–75]. Shock velocity vs particle velocity data on Ti and Zr show discontinuities at 17.5 and 26 GPa respectively, and the source of these discontinuities has been the topic of considerable controversy in the literature[73]. Various proposals are critically examined in the light of total energy

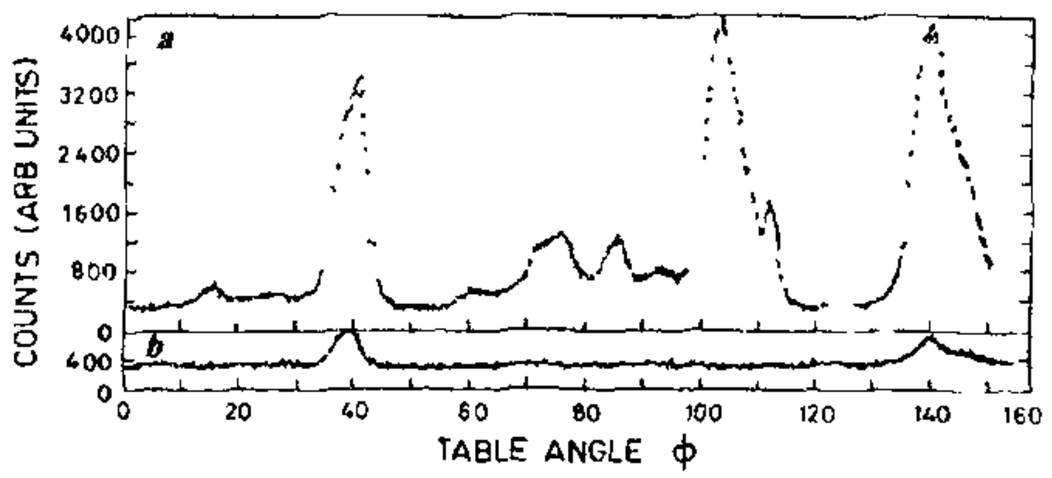

Figure 4. *a*, Rocking curves for $(10\bar{1}1)_\omega$ and $(11\bar{2}0)_\omega$ reflections. *b*, Rocking curves for second-order reflection $(22\bar{4}0)_\omega$; the peaks corresponding to $(20\bar{2}2)_\omega$ reflection are absent. [Ref. 72]

calculations and DAC-based X-ray diffraction results by Gyanchandani *et al.* Their predicted transitions for Zr are shown in Figure 5. From this they concluded that the 26 GPa discontinuity in Zr is due to the ω–β transition, which is aided by shear band heating. This predicted transformation has been recently observed through an X-ray diffraction study at high pressures[76]. In Ti they found no possible cause of a discontinuity and it is heartening to note that the recent experiments carried out at Los Alamos also do not show any discontinuity. In recent calculation on Hf they have shown that the observed phase transitions[77] α–ω at 38 GPa and ω–β at 71 GPa are also related to *d*-band occupancy.

Rare earths and actinides

Rare earths and actinides are characterized by a gradual filling of the 4*f* and 5*f* shells respectively. For most of the rare earths the 4*f* shell is located deep within the atom which implies that the outer electronic structure of various elements is very similar, resulting in a systematic gradation of properties in the solid phase. However, this is quite different in the actinides where *f* electrons participate in cohesion and even when

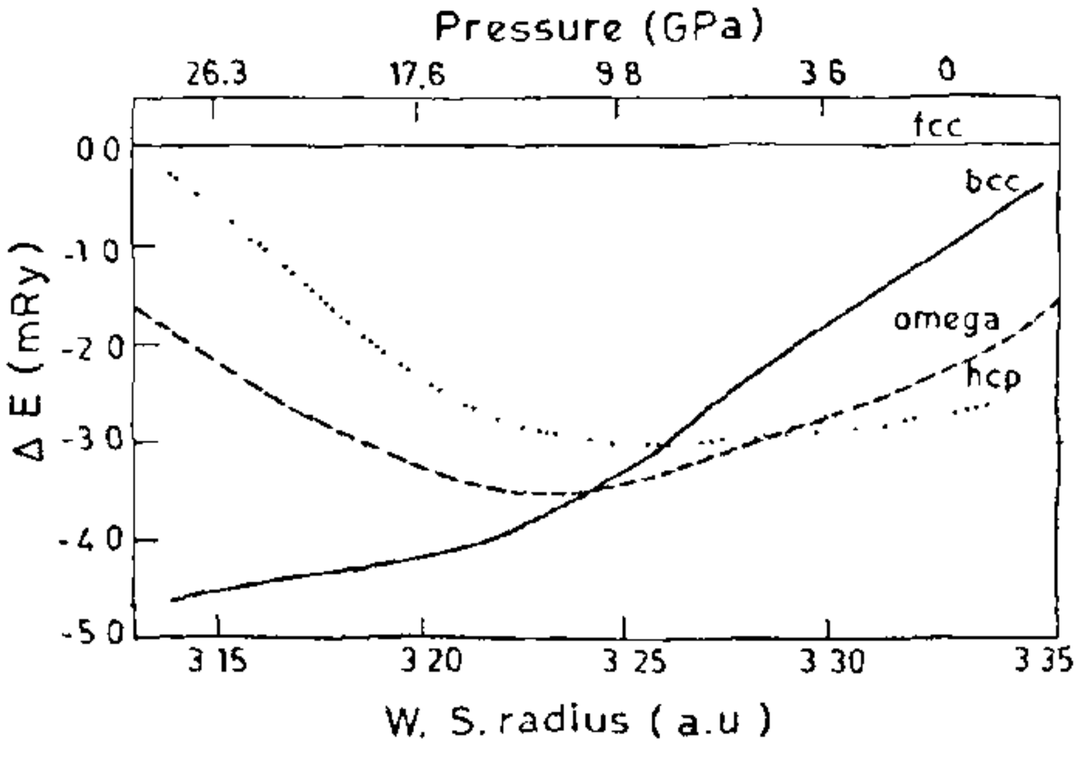

Figure 5. Calculated structural energy differences for Zr. [Ref. 67]

localized they form a substantial part of an actinide atom.

Rare earths show a well-defined sequence of transitions under pressure: hcp–Sm-type–dhcp–fcc. Johansson and Rosengren[78] established an empirical relation between the crystal structure and the fraction of occupied volume by defining an 'effective' ion core. This suggests that an increase in pressure simulates a lighter element. This correlation was given a quantitative justification by Duthie and Pettifor[79] in terms of *d*-band occupancy and its variation with pressure. It was shown that the structural stability is related to *d*-band occupancy Nd in the following way: Nd < 1.7 hcp; 1.7 < Nd < 2.3 Sm-type; 2.3 < Nd < 2.6 dhcp and Nd > 2.6 fcc. Therefore 4*f* electrons are irrelevant to the complex sequence of structures. The study of Y up to 34 GPa further confirmed this[80]. Y is a 4*d* transition metal with no 4*f* electrons but under pressure it shows the same sequence of transitions hcp–Sm-type–dhcp. So it appears that the observed sequence of structures of rare earths under pressure is a direct consequence of $s \rightarrow d$ transfer.

When the trivalent rare earths La, Pr, Nd, etc. are pressurized beyond the fcc phase, they show a continuous distortion of the fcc lattice[81]. This structure is also seen in Cf and Am of the actinide series[82,83]. This distorted fcc structure was shown by Vohra *et al.*[81] to belong to a trigonal space group $P3_221$ with hexagonal layers modulated along the c axis, with $C = 3\lambda$, λ being the wavelength of the modulation wave. This is shown in Figure 6. This phase evolves from fcc by softening of a zone boundary longitudinal phonon mode corresponding to the L point in the Brillouin zone.

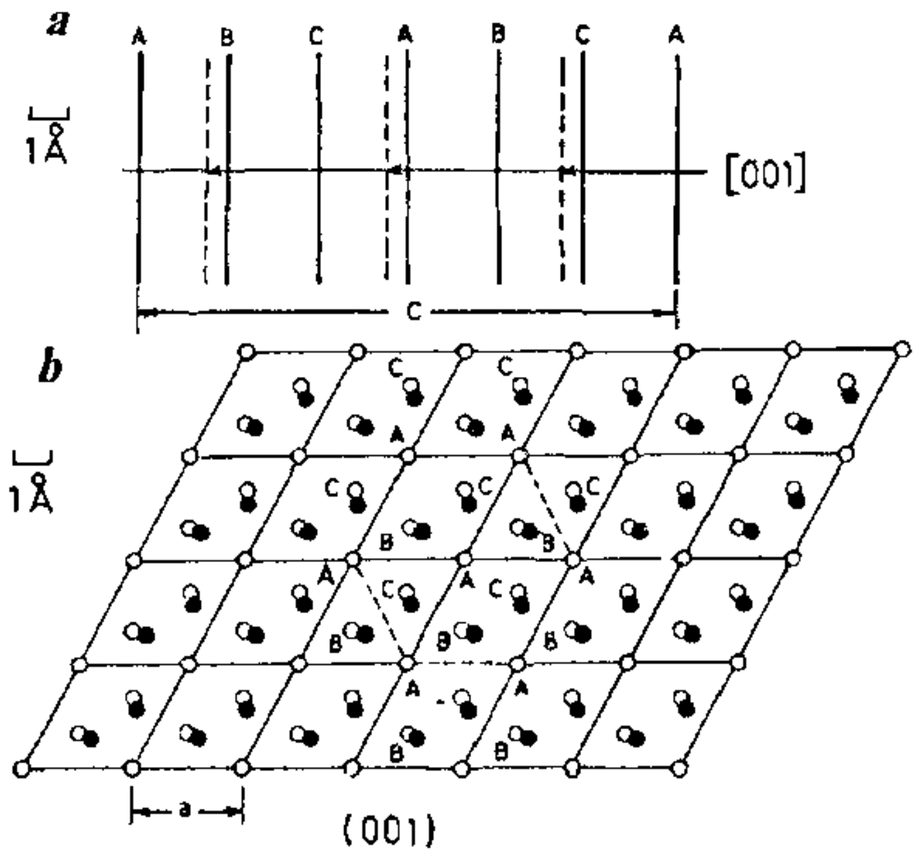

Figure 6. The proposed distorted fcc structure for rare earths at high pressures. *a*, Periodic modulation of the hexagonal layers along the c axis. The dashed lines represent the new positions. *b*, The relative shifts of the hexagonal layers in the basal plane. The B and C layers are sheared with respect to the A layer; the new atom position for these layers is indicated by filled circles. [Ref. 81]

This work showed that the triple-hexagonal close-packed structure proposed for this phase[84] is incorrect. Sikka *et al.*[85,86], through their X-ray diffraction results on $La_{0.8}Th_{0.2}$ stabilized in Pr(III) phase, showed conclusively that the distorted fcc phase is indeed the modulated hexagonal structure discussed above.

While $s \rightarrow d$ transfer is the source of structural sequence in rare earths this may also bring about electronic transitions without a structural change. One such example studied by Vijayakumar *et al.*[87] is the $La_{1-x}Th_x$ alloy system. This alloy was stabilized in fcc ($x = 0.1$) and distorted fcc ($x = 0.2$) to study the anomaly in the resistance observed at about 2.5 GPa in pure La (dhcp). They showed that the existence of this anomaly is independent of the phase, though the alloying lowers the pressure of the transformation. Further, the transformation pressure depends only on total conduction electron density parameter[87] r_s. These observations suggest that the 2.5-GPa transition in La is essentially electronic and may be the Lifshitz–Dagen's transition.

The crystal structures of actinides are much more complicated and diversified when compared to rare earths. So one finds many crystal structures which are quite distorted and unique in the periodic table. This is because the 5*f* electrons in lighter actinides are itinerant in character and play a part in stabilizing the structures. Further these structures are such that there are many atoms in the unit cell (α-Pu has 16 atoms per cell) and not all the atoms are of the same size as shown by short and long bond lengths. But for heavier actinides 5*f* electrons become substantially localized. This change in character takes place between Pu and Am. So one should expect that actinides from Am onwards would show a typical rare earth behaviour. This is confirmed by the appearance of dhcp structure in Am, Cm, Bk and Cf. However, pressure delocalizes the 5*f* and the α-U structure again appears at high pressures[88]. Because of the inherent difficulty of radioactive contamination of the cell, we have not carried out experimental work in this series so far.

It may also be mentioned that it had been suggested by Vohra *et al.*[89] that *f* electrons even in early actinides may become localized at high temperatures (close to melting). This conclusion is based on unusually large thermal expansion coefficients in Np and Pu along with their observation of (high-temperature phase of Np) β-Np structure in trivalent, 3*d*-transition metal, Sc under pressure. A reanalysis by Sikka[90] shows that the atomic volumes of the high temperature bcc phases of U, Np and Pu are considerably lower than the ones required by theory for localizing *f* electrons. This warrants an alternative interpretation for the so-called β-Np phase of Sc. It was shown that the Sc structure may be an intermediate between fcc- and hcp-like structures. This structure gives a diffraction pattern identical to that observed from the high-pressure phase of Sc, mistaken-

ly identified as β-Np. So the conclusion is that f electrons continue to be delocalized for U, Np and Pu even at high temperatures. Pa may, however, be an exception.

Dynamic pressures

To carry out experiments at high-strain rates through dynamic pressure loading under shocks, Gupta *et al.*[91] have set up a compressed gas-gun facility at Trombay (see cover picture). This is a convenient way to carry out laboratory experiments with planar shocks. In this the projectile is accelerated to a chosen velocity by releasing the pressurized gas from the breech. The projectile, with the impactor mounted on the nose, flies through a barrel (diameter 63.5 mm) to impact the target material to generate a shock wave. The projectile could be accelerated up to 1.2 km sec^{-1} to generate a peak pressure of up to 40 GPa, depending upon the impedances of the impactor and the target. A slot in the barrel with a corresponding key in the projectile inhibits any possible rotation of the projectile, permitting impact of inclined parallel plates to study compressive shear phenomena. Just before the impact, the velocity of the projectile is measured by noting the time of flight between two consecutive pairs of shorted pins: the relative tilt of the impactor with respect to the target is also very accurately measured on impact. The shock profiles, the shock velocity and the particle velocity can be obtained with appropriate measurements through manganin, Yb or electromagnetic gauges. The signal from the gauge is recorded using fast oscilloscopes.

Various kinds o phenomena like phase transitions, dynamic yielding or stress/high-strain rate-induced chemical reactions show up as some break or anomaly in the shock Hugoniot. But essentially those phenomena will be observed where there is a substantial change within a microsecond, the typical time duration of a shock wave. We plan to study phase transformations under shock conditions in conjunction with static measurements, particularly the effects of shear on kinetics of phase transitions.

Our group has also carried out extensive theoretical investigations in this area which are well documented in the review article by Godwal *et al.*[3] The starting point is invariably the total energy calculations using a variety of band structural methods to construct a zero-degree isotherm of the solid. Since the temperature and the pressure are tied together in the shock Hugoniot one has to incorporate the effect of temperature. This is typically evaluated using the Debye–Mie–Gruneisen model, i.e.

$$P_T = \frac{\gamma(V)}{V} E_T,$$

where P_T and E_T are the pressures and internal energy associated with lattice vibrations ($E_T \sim 3\ K_B T$ for $T > \theta_D$) and $\gamma(V)$ is the Gruneisen parameter. The volume variation of γ can be evaluated from the zero-degree isotherm through various prescriptions[3]. In this way one can compute the Hugoniot for any material. Some typical examples from the work of our group are: Al (ref. 92), Th (ref. 93), and Pb ref. (94) for EOS in the normal region ($P < 500$ GPa). In the high density region ($P > 10{,}000$ GPa), Thomas–Fermi–Dirac theory is adequate for constructing the EOS. But the intermediate region (between 500 GPa and 10,000 GPa) is difficult to treat.

In this intermediate region, the situation becomes complex because of phenomena like pressure and thermal ionization of core states. Godwal and Sikka[95] showed that one can use the modified Saha ionization theory to incorporate these aspects in an appropriate manner. In this way Godwal *et al.*[96] constructed the Hugoniot of Al up to 2000 GPa and this is shown in Figure 7. The experimental point, shown by a solid circle, due to Volkov *et al.*[97], came after the calculations and fell exactly on the predicted Hugoniot. The data of Mitchell and Nellis[98], which also came after our calculations, are also in perfect agreement with the predictions[99,100].

The modified Saha ionization theory has also been used by Godwal[101] to study the valence transitions under pressure in Eu and Yb. The calculation predicts that in Eu, $4f$ delocalization starts at $V/V_0 = 0.55$, while for Yb it does so at 0.75, in reasonable agreement with experimental observations. Shock wave studies on Yb

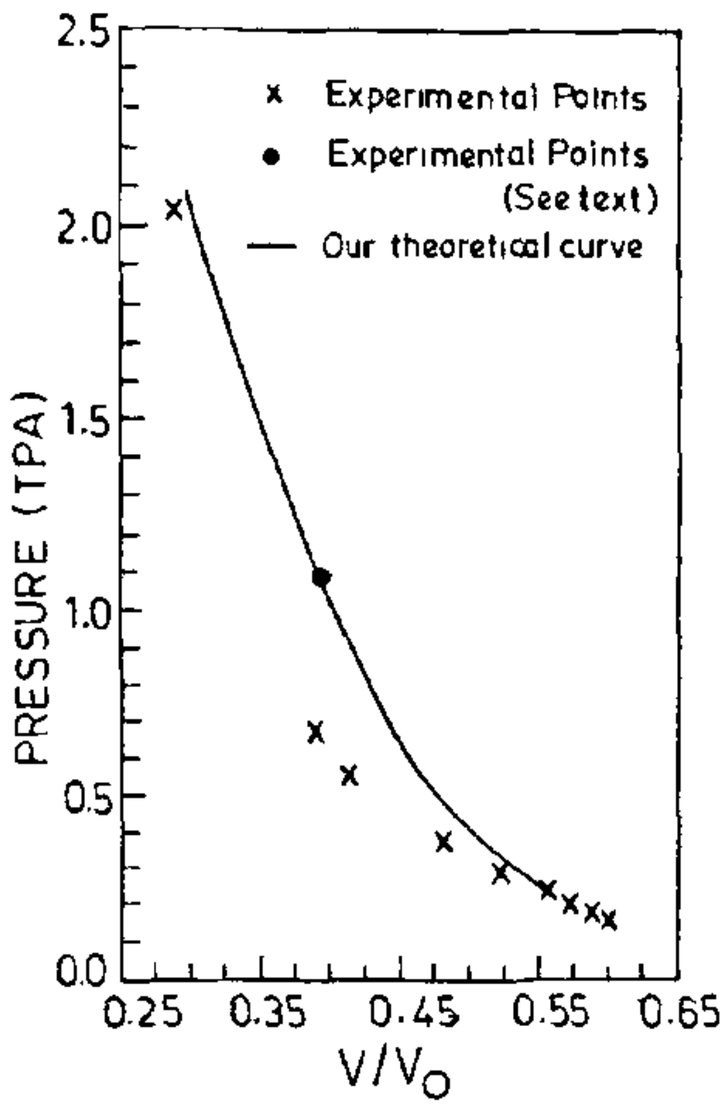

Figure 7. The computed shock Hugoniot of Al up to the intermediate range [Ref 96]

show a discontinuity in the slope of shock velocity–particle velocity curve with stiffening of Hugoniot[102,103] at $V/V_0 = 0.58$. Gyanchandani *et al.*[104] examined the cause of this stiffening. From the comparison of Hugoniot with the existing X-ray diffraction data, L_{III}-absorption edge measurements and computed Hugoniot from LMTO band structure method, they showed that the cause of this stiffening in this material is the $2 \rightarrow 3$ valence transition mentioned above. Comparison of calculations and experimental data is shown in Figure 8. Various other issues related to EOS, like the physical significance of (largely) linear relationship between shock and particle velocity, have also been investigated theoretically[105]. It was shown recently that in the presence of $s \rightarrow d$ transition the universal EOS requires the incorporation of higher order terms[106] and also that the universal EOS fits the data better than the Birch–Murnaghan equation[107]. Some of the recent EOS calculations carried out by members of our group are on Re (ref. 108), Pb (ref. 109), Au (ref. 110) and Mo (ref. 111).

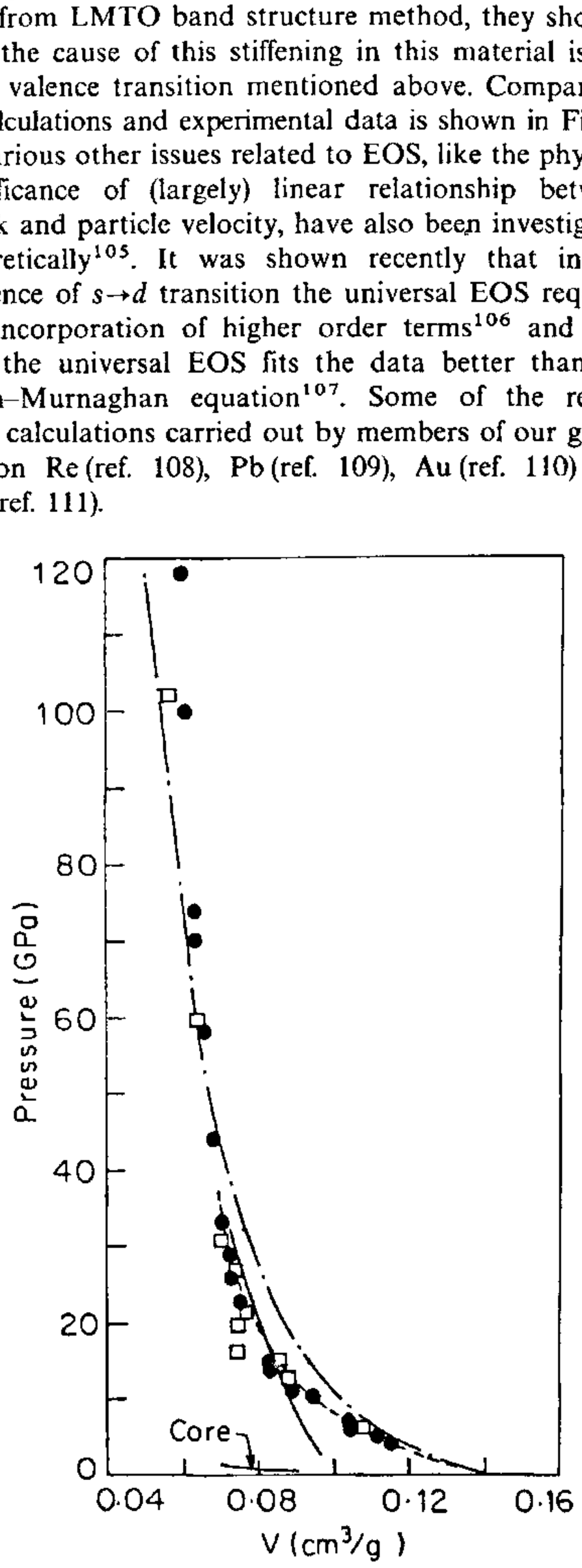

Figure 8. Observed and calculated Hugoniots for Yb. [Ref. 104; □ and ● are data from refs. 102 and 103] solid line is the calculated Hugoniot for trivalent and dot-dash represents the calculated Hugoniot for divalent state of Yb. Dashed line is the Hugoniot constructed from 300-K isotherm from the data of Takemura and Syassen[103].

Another problem of considerable significance to the field of high pressures is the response of ruby R lines to external stresses. Its significance for static pressures is primarily as a pressure marker[112]. Recent studies of response of R lines to shock compressive and tensile loading along oriented crystals below Hugoniot elastic limit (HEL) showed shifts to be highly anisotropic, nonlinear and anomalous compared to the response in the settings of DAC[113,114]. This necessitated an understanding of this problem in detail at the microscopic level. Therefore, a comprehensive theory for quantitative predictions of response of R lines under uniaxial strain (tension and compression), uniaxial stress and hydrostatic pressure for different crystallographic orientations was developed by Sharma and Gupta[115] at Washington State University. A symmetry-adapted representation of various loading conditions, in conjunction with crystal field theory, is used to relate the R-line shifts to external deformation. Parameters were evaluated from shock-wave compression data along c and a axes. Without any further adjustments of parameters all the known experimental results to date have been quantitatively explained. It is worth pointing out that this is the only theoretical study which deals with the response of R lines under most general stress conditions. Other known theoretical attempts deal with the idealized isotropic compression of ruby which in fact does not represent even the strain state due to hydrostatic pressure[115]. Generalization of these has not been attempted to include more general strain state. Typical first-principle attempts to explain the red shift under hydrostatic pressure give results which are an order of magnitude higher than the observed shifts. In addition to the general theory, the utility of the point-ion model in predicting shifts under hydrostatic conditions and the need to carry out new absorption-band measurements was also established[116]. Further, the significance of spin–orbit interaction in predicting lifetime of R lines was shown through a successful explanation of lifetime variations under pressure[117]. This work suggests the use of oriented chips of ruby in DAC for pressure calibration. In the absence of this, the R_2 line should be used as a marker for estimating the overall compression. This prediction is verified by a reanalysis of experimental data of shocks along the a axis of ruby[118]. Further, this theoretical development provides the first significant step towards an understanding of shock deformation in crystalline solids beyond yielding by optical measurements. Recent results of such studies are encouraging[119].

Future directions

With the accessibility of static pressures higher than those at the centre of the earth by DAC, it is likely that studies of materials of geophysical interest, coupled with

laser heating[120,121] and synchrotron radiation, will be an area of active research. At these pressures (>400 GPa), one can expect to see the beginning of pressure ionization of core states and some consequent surprises. However, central to further studies of this kind is the question as to what could be highest pressure achievable under static conditions. Calculations show that the diamond is stable[122] against most well-known phase transitions (to bcc, fcc, hcp, β-tin, etc.) up to well over 2000 GPa. A possible pressure-induced metallization is also expected to be higher than at about 1000 GPa. So the highest pressures are likely to be restricted by the plastic yield limit. It is estimated that perfect diamonds will be able to sustain pressures higher than 500 GPa before yielding[123]. It is possible that a high-quality diamond ceramic fabricated from the sintering of fine diamond powder may provide even higher yielding strengths[124]. A glassy diamond ceramic of this kind gives the highest values of shear strengths compared to any kinds of diamonds tested[125]. The study of materials at more easily accessible pressures (say, <50 GPa) will continue to be as exciting as ever on newer and newer materials with a variety of techniques. Very much more remains to be done within this range as the recent discovery of amorphization under pressure shows.

In the area of studies of materials under shock loading, barring a few, most of the studies are of continuum nature. So the questions as to how shocks propagate and as to what the state of matter is immediately behind the shock front are pretty much open questions[126], though a few attempts by flash X-ray diffraction have been made by Johnson and Mitchell[127], and by Whitlock and coworkers[128]. It is expected that more experiments of this kind will provide very valuable information. Optical experiments, like the one on shocked ruby, beyond Hugoniot elastic limit hold forth significant promise particularly due to their time-resolved nature[119]. Interaction of theory and experiments in this region may provide insight into the dynamic stress relaxation processes behind the shock front. In the context of general shock wave research, the measurement of precise temperatures is a crying need. Presently even the improved pyrometric method[129] gives temperatures which are substantially higher than expected even at low pressures (<100 GPa) range. The area of study of kinetics of phase transitions under shocks is an interesting and challenging one and some information could be derived from accurate profile measurements. The difference between the kinetics under shock loading and that under static pressures may not be due to nonhydrostaticity and temperatures alone. These are likely to be intertwined with the fact that the shock jump in pressure is essentially a nonequilibrium phenomenon which may play a deciding role.

On the theoretical side, first-principle molecular-dynamical calculations[130] may contribute significantly to the understanding of phenomena at high pressures as a recent calculation of melting curve of diamonds has shown[131]. Similar attempts are also being made to unravel the complexities of shock propagation in solids[132,133]. It can be hoped that this interaction of theory and experiments will open up new vistas in the area of high-pressure physics. To summarize, the area of high-pressure research continues to be full of a great deal of excitement.

1. Chidambaram, R. and Ramanna, R., Proc Tech Commun PNE IV Vienna, International Atomic Energy Agency, 1975, p. 421
2. Chidambaram, R., Sikka, S. K. and Gupta, S. C., *Pramana—J Phys*, 1985, **24**, 245
3. Godwal, B. K., Sikka, S. K. and Chidambaram, R., *Phys Rep.*, 1983, **102**, 121.
4. Ross, M., *Rep Progr. Phys*, 1985, **48**, 1.
5. Skelton, E. F., Webb, A. W., Qadri, S. B., Carpenter, E. R., Jr Harford, M. Z., Lubitz, P. and Twigg, M., *High Pressure Res.*, 1990, **5**, 914
6. Yamaoka, S. *et al*, *Physica*, 1986, **B139&140**, 668.
7. Sankaran, H., Sikka, S. K., Sharma, S. M. and Chidambaram, R., *Phys Rev.*, 1988, **B38**, 170.
8. Sankaran, H., Sharma, S. M., Sikka, S. K and Chidambaram, R., *Pramana—J Phys*, 1990, **35**, 177; Mishima, O., Calvert, L. D. and Whalley, E., *Nature*, 1984, **310**, 393, Fujii, Y., Kowaka, and Onodera, A., *J. Phys*, 1985, **C18**, 789; Chaplot, S. L. and Mukhopadhyay, R., *Phys Rev.*, 1986, **B33**, 5099, Hemley, R. J., Jephcoat, A. P., Mao, H. K., Ming, L. C. and Manghnani, M. H., *Nature*, 1988, **334**, 52; Williams, Q. and Jeanloz, R., *J. Chem. Phys.*, 1989, **91**, 5910, Williams, Q., Knittle, K., Reichlin, R., Martin, S and Jeanloz, R., *J Geophys Res.*, 1990, **B95**, 21549
9. Hirschfelder, J. O., Curtiss, C. F. and Bird, R. B., *Molecular Theory of Gases and Liquids*, Wiley, New York, 1964, Chap 4.
10. McMahan, A. K., *Phys Rev.*, 1984, **B29**, 5982, Pauling, L., *Proc Natl. Acad. Sci. USA*, 1989, **86**, 1431, Vijayakumar, V., Sikka, S. K and Olijnyk, H., *Phys. Lett*, 1991, **A152**, 353.
11. Gupta, S. C., Sikka, S. K., Godwal, B. K. and Chidambaram, R., *Current Trends in the Physics of Condensed Matter* (ed. Yussouff, M.), World Scientific, Singapore, 1987, p. 46
12. Sankaran, H., Sharma, S. M. and Sikka, S. K., *Phys. Rev.*, 1986, **B33**, 3543.
13. Vijayakumar, V., Godwal, B. K. and Sikka, S. K., *Phys. Rev*, 1989, **B32**, 4212
14. Mao, H. K., Hemley, R. J. and Hanfland, M., *Phys Rev. Lett.*, 1990, **65**, 484.
15. Takemura, K., Minomura, S., Shimomura, O. and Fujio, Y., *Phys Rev Lett*, 1980, **45**, 1881.
16. Lorenzana, H. E., Silvera, I. F. and Goettel, K. A., *Phys Rev. Lett.*, 1990, **64**, 1939
17. Chancham, H. and Louie, S. G., *Phys. Rev. Lett.*, 1991, **66**, 64.
18. Eggert, J. H *et al*, *Phys Rev. Lett.*, 1991, **66**, 193
19. Ruoff, A. L. and Vanderborgh, C. A., *Phys. Rev Lett*, 1991, **66**, 754
20. Reichlen, R., Ross, M., Martin, S. and Goettel, K. A., *Phys Rev Lett*, 1986, **56**, 2858.
21. Goettel, K. A., Eggert, J. H., Silvera, F. and Moss, W. C., *Phys. Rev. Lett.*, 1989, **62**, 665, Reichlin, R., Brister, K. E., McMahan, A. K., Ross, M., Martin, S., Vohra, Y. K and Ruoff, A. L., *Phys Rev. Lett.*, 1989, **62**, 669

22 Chacham, H, Zhu, X. and Louie, S. G., *Europhys. Lett.*, 1991, **14**, 65.
23. Sharma, S. M., Vijayakumar, V., Sikka, S. K. and Chidambaram, R., *Pramana—J. Phys.*, 1985, **25**, 75.
24. Sankaran, H., Sharma, S. M., Sikka, S. K. and Chidambaram, R, *Pramana—J. Phys.*, 1986, **27**, 835.
25. Heremans, K., *High Pressure Res*, 1990, **5**, 743.
26. Heremans, K. and Bormans, M., *Physica*, 1986, **B139**, and **B140**, 870.
27. Vohra, Y. K., Vijayakumar, V., Godwal, B K., Sikka, S K. and Chidambaram, R., *Rev. Sci. Instrum.*, 1984, **55**, 1593.
28 Sankaran, H., Sikka, S. K., Sharma, S. M. and Chidambaram, R., *Proc. Solid State Symp. Bhopal*, 1988, **C31**, 390.
29. Huber, G., Syassen, K. and Holzapfel, W. B., *Phys. Rev*, 1977, **B15**, 5123.
30. Sikka, S. K., Sankaran, H., Sharma, S. M., Vijayakumar, V., Godwal, B K. and Chidambaram, R., *Indian J. Pure Appl. Phys*, 1989, **27**, 472.
31. Hafner, J. and Heine, V., *J. Phys.*, 1983, **F13**, 2479.
32. Vijayakumar, V., Sharma, S. M., Sikka, S. K. and Chidambaram, R., *J. Phys.*, 1986, **F16**, 831.
33. Sharma, S. M., Sankaran, H., Sikka, S. K. and Chidambaram, R., *Phys. Rev.*, 1987, **B36**, 7730.
34. Lindgard, P. A. and Mouritsen, O. G., *Phys. Rev. Lett.*, 1986, **57**, 2458.
35. Schulte, O. and Holzapfel, W. B., *Phys. Lett.*, 1988, **A131**, 38.
36. Barrett, C. S., *Acta Crystallogr.*, 1956, **9**, 671.
37. Berliner, R., Fajen, O., Smith, H G. and Hitterman, R. A., *Phys. Rev.*, 1989, **B40**, 12086; Berliner, R. A. and Werner, S. A., *Phys. Rev*, 1986, **B34**, 3586; Smith, H. G., Berliner, R., Jorgensen, J. D. and Trivisonno, J., *Phys. Rev.*, 1991, **B43**, 4524.
38. Berliner, R., Smith, H. G., Copley, J. R. D. and Trivisonno, J. Annual Report of Rutherford Laboratory, 1990, unpublished,
39. Sankaran, H, Sharma, S. M. and Sikka, S. K., *Phys. Rev. Lett.*, (communicated).
40. Mao, H. K. *et al.*, *Phys. Rev. Lett.*, 1990, **64**, 1749.
41. Olijnyk, H., Sikka, S. K. and Holzapfel, W. B., *Phys. Lett.*, 1984, **A103**, 137.
42. Sharma, S. M. and Sikka, S. K., *J. Phys. Chem. Solids*, 1985, **46**, 477.
43. Ivanov, A. S., Rumiantsev, A. Yu., Metrofanov, N. L. and Alba, M., To appear in the Proceedings of International Conference on Neutron Scattering, 1991, Bombay (in *Physica* B).
44. Hazen, R. M. and Finger, L. W., *Am. Sci.*, 1984, **72**, 143; *Sci. Am.*, 1985, **252**, 110.
45. Moffatt, W. G., Pearshall, G. W. and Wulff, J., *The Structure and Properties of Materials*, Wiley Eastern, 1980, vol. 1, chap. 5.
46. Bansal, M. L., in Proc. Third National Seminar on Feroelectrics and Dielectrics, India, 1984, p. 77.
47. Sandhya Bhakhay-Tamhane and Sequeira, A., *Ferroelectrics*, 1986, **69**, 241.
48. Sankaran, H, Sharma, S. M. and Sikka, S. K., *Solid State Commun.*, 1988, **66**, 7.
49. Melo, F. E. A., Lemos, V., Cerdeira, F. and Filho, J. M., *Phys. Rev.*, 1987, **B35**, 3633.
50. Arora, A. K. and Sakuntala, T., *Solid State Commun.*, 1990, **75**, 855.
51. Hemley, R. J., Jephcoat, A. P., Mao, H. K., Ming, L. C. and Manghnani, M. H., *Nature*, 1988, **334**, 52, Hazen, R. M., Finger, L. W. and Hemley, R. J., *Solid State Commun.*, 1989, **72**, 507.
52. Sankaran, H., Sikka, S. K. and Chidambaram, R., *High Pressure Res.*, 1990, **4**, 393.
53. Thong, N. and Schwarzenbach, *Acta Crystallogr.*, 1979, **A35**, 658
54 Kruger, M. B. and Jeanloz, R., *Science*, 1990, **249**, 647.
55. Deb, S. K. *et al*, (to be published).
56. Pruzan, Ph, Chervin, J C., Thiery, M. M., Itie, J. P. and Besson, J. M., *High Pressure Res*, 1990, **3**, 215.
57. Chaplot, S. L. and Sikka S. K., Solid State Physics Symp., DAE, Bombay, 1990, **C33**, 328.
58. Chaplot, S. L. and Sikka, S K., (manuscript in preparation).
59. Pettifor, D. G., *J. Phys.*, 1970, **C3**, 367, and in *Metallurgical Chemistry* (ed Kubaschewski, O), Her Majesty's Stationary Office, London, 1972; and *Comput Coupling Phase Diagrams and Thermochem*, (CALPHAD) 1977, **1**, 305.
60. Williams, A. R. (unpublished) and quoted in ref. Miedema, A. R. and Niessen, A K., *CALPHAD*, 1983, **7**, 27.
61. Skriver, H. L., *Phys. Rev.*, 1985, **B31**, 1909.
62. McMahan, A. K., *Physica*, 1986, **139** and **B140**, 31.
63. Olijnyk, H. and Holzapfel, W. B, *Phys. Rev.*, 1985, **B31**, 4682.
64. Sikka, S. K., Vohra, Y. K. and Chidambaram, R., *Progr. Mat. Sci.*, 1982, **27**, 245.
65. Vohra, Y. K., Sikka, S. K. and Chidambaram, R., *J. Phys.*, 1979, **F9**, 1771.,
66. Sharma, S. M, Sikka, S. K. and Chidambaram, R., *Positron Annihilation* (eds Jain, P. C., Singru, R. M. and Gopinathan, K. P.), World Scientific, Singapore, 1985, p. 52.
67. Gyanchandani, J. S., Gupta, S. C., Sikka, S. K. and Chidambaram, R, *High Pressure Res.*, 1990, **3**, 472.
68. Usikov, M. P. and Zilbershtein, V. A., *Phys. Status Solidi*, 1973, **A19**, 53.
69. Vohra, Y. K., Sikka, S. K., Menon, E. S. K. and Krishnan, R., *Acta Metall.*, 1980, **28**, 683.
70 Vohra, Y. K., Sikka, S. K. and Chidambaram, R., *Bull Mater. Sci.*, 1981, **2**, 109.
71. Vohra, Y. K., Menon, E. S. K., Sikka, S. K. and Krishnan, R., *Acta Metall.*, 1981, **29**, 457.
72. Gupta, S. C., Sikka, S. K. and Chidambaram, R., *Scr. Metall.*, 1985, **19**, 1167.
73. Gyanchandani, J. S., Gupta, S. C., Sikka, S. K. and Chidambaram, R., *Shock Compression of Condensed Matter*—1989, (eds Schmidt, S. C., Johnson, J. N. and Davison, J. W), North Holland, 1990, p. 131.
74 Gyanchandani, J. S., Gupta, S. C., Sikka, S. K. and Chidambaram, R., *J. Phys. Condens. Matter.*, 1990, **2**, 301.
75. Gyanchandani, J. S., Gupta, S. C., Sikka, S. K. and Chidambaram, R., *J. Phys. Condens. Matter*, 1990, **2**, 6457.
76. Xia, H., Dulcos, S. J., Ruoff, A. L. and Vohra, Y. K., *Phys. Rev. Lett.*, 1990, **64**, 204.
77. Xia, H., Parthasarathy, G., Luo, H., Vohra, Y. K. and Ruoff, A., *Phys. Rev*, 1990, **B42**, 6736.
78 Johansson, B. and Rosengren, A., *Phys. Rev.*, 1975, **B11**, 1367, 2836.
79. Duthie, J. C. and Pettifor, D. G., *Phys. Rev. Lett*, 1977, **38**, 564.
80. Grosshans, W. A., Vohra, Y. K. and Holzapfel, W. B., *Phys. Rev. Lett.*, 1982, **49**, 1572.
81. Vohra, Y. K., Vijayakumar, V., Godwal, B. K. and Sikka, S. K., *Phys. Rev.*, 1984, **B30**, 6205.
82. Benedict, U., Peterson, J. R., Haire, R. G. and Dufour, C., *J. Phys.*, 1984, **F14**, L43
83. See references 37–47 in review by Benedict, U, 1984, ref. 88.
84. Smith, G. S. and Akella, J., *Phys Lett.*, 1984, **A105**, 132.
85. Sikka, S. K., Godwal, B. K. and Vijayakumar, V., *Phys. Lett.*, 1985, **A108**, 83.
86. Sikka, S. K. and Vijayakumar, V., *Physica*, 1986, **B144**, 23.
87. Vijayakumar, V., Sikka, S K., Godwal, B. K. and Chidambaram, R., *Physica*, 1986, **139** and **B140**, 407.
88. Benedict, U., *J. Less-Common Met.*, 1984, **100**, 153
89. Vohra, Y. K., Grosshans and Holzapfel, W. B., *Phys. Rev*, 1982, **B25**, 6019; Vohra, Y. K. and Holzapfel, W B, *Phys Lett.*, 1982, **A89**, 149.
90 Sikka, S. K, *High Pressure Res.*, 1990, **2**, 289.
91. Gupta, S. C., Gyanchandani, J. S, Sikka, S. K, Chidambaram, R, Agarwal, R. G. and Kakodkar, A K., *Solid State Phys.*,

Symposium, DAE, Bombay, 1990, 33C, 445.
92. Godwal, B. K., Sikka, S. K. and Chidambaram, R., *Phys. Rev.*, 1979, **B20**, 2362.
93. Godwal, B. K. and Sikka, S. K., *J. Phys.*, 1982, **F12**, 655.
94. Godwal, B. K., Sikka, S. K. and Chidambaram, R., *Pramana—J. Phys.*, 1987, **29**, 93.
95. Godwal, B. K. and Sikka, S. K., *Pramana—J. Phys.*, 1977, **8**, 217.
96. Godwal, B. K., Sikka, S. K. and Chidambaram, R., *Phys. Rev. Lett.*, 1981, **47**, 1144.
97. Volkov, A. P., Voloshin, N. P., Vladimira, A. S., Nogin, V. N., and Simonenko, V. A., *Plasma Zh. Eksp. Theor. Fiz.*, 1980, **31**, 623. [*JETP Lett.*, 1980, **31**, 588].
98. Mitchell, A. C. and Nellis, W. J., *J. Appl. Phys.*, 1981, **52**, 3363.
99. Sikka, S. K., *Shock Waves in Condensed Matter* (ed. Gupta Y. M.) Plenum New York, 1986, p. 71.
100. Sikka, S. K., Physics of Condensed Matter at High Pressures, 11-29 August 1986, International Centre for Theoretical Physics; unpublished.
101. Godwal, B. K., *Phys. Rev.*, 1983, **A28**, 1103.
102. Gust, W. H. and Royce, E. B., *Phys. Rev.*, 1973, **B8**, 3595.
103. Carter, W. J., Fritz, J. N., Marsh, S. P. and McQueen, R. G., *J. Phys. Chem. Solids*, 1975, **36**, 741, Takemura, K. and Syassen, K., *J. Phys.*, 1985, **F15**, 543.
104. Gyanchandani, J. S., Gupta, S. C., Sikka, S. K. and Chidambaram, R., *Shock Waves in Condensed Matter 1987*, (eds. Schmidt, S. C. and Holmes N. C.), Elsevier Science, 1988, p. 147.
105. Sikka, S. K. and Godwal, B. K., *Solid State Commun.*, 1981, **38**, 949.
106. Sikka, S. K., *Phys. Rev.*, 1988, **B38**, 8463.
107. Sikka, S. K., *Phys. Lett.*, 1989, **A135**, 129.
108. Sikka, S. K. and Vijayakumar, V., *Phys. Rev.*, 1988, **B38**, 10926.
109. Lui, A. Y., Garcia, A., Cohen, M. L., Godwal, B. K., *Jeanloz R., Phys. Rev.*, 1991, **B43**, 1795.
110. Godwal, B. K. and Jeanloz, R., *Phys. Rev.*, 1989, **B40**, 7501.
111. Godwal, B. K. and Jeanloz, R., *Phys. Rev.*, 1990, **B41**, 7440.
112. Jayaraman, A., Rev. *Mod. Phys.*, 1983, **55**, 65.
113. Horn, P. D. and Gupta, Y. M., *Appl. Phys. Lett.*, 1986, **49**, 856, *Phys. Rev.*, 1989, **B39**, 973.
114. Shen, X. A. and Gupta, Y. M., *Shock Compression of Condensed Matter—1989* (eds Schmidt, S. C., Johnson, J. N. and Davison, L. W.), Elsevier Science, 1990, p. 893.
115. Sharma, S. M. and Gupta, Y. M., *Phys. Rev.*, 1991, **B43**, 879.
116. Sharma, S. M. and Gupta, Y. M., *Phys. Rev.*, 1989, **B40**, 3329.
117. Sharma, S. M. and Gupta, Y. M., *Appl. Phys. Lett.*, 1989, **54**, 84.
118. Gupta, Y. M. and Shen, X. A., *Appl. Phys. Lett.*, 1991, **58**, 583.
119. Gupta, Y. M., Personal communication.
120. Bassett, W. A., *Scr. Metall.*, 1988, **22**, 157.
121. Jeanloz, R. and Heinz, D. L., *J. Phys.*, 1984, **8**, 83.
122. Yin, M. T. and Cohen, M. L., *Phys. Rev. Lett.*, 1983, **50**, 2006.
123. Jayaraman, A., *Sci. Am.*, 1984, **250**, 42.
124. Bundy, F. P., *Physica*, 1986, **139** and **B140**, 42.
125. Bundy, F. P., *J. Chem. Phys.*, 1963, **38**, 631.
126. Chidambaram, R., *Bull. Mater. Sci.*, 1984, **6**, 633.
127. Johnson, Q. and Mitchell, A., *Phys. Rev. Lett.*, 1972, **29**, 1369, and the references therein.
128. Whitlock, R. R., Wark, J. S. and Kiehm, G., *Shock Compression of Condensed Matter—1989* (ed. Schmidt, S. C., Johnson, J. N. and Davison, L. W.), Elsevier Science, 1990, p. 897 and p. 901.
129. Perez, M. and Costeraste, J., *Shock Waves in Condensed Matter—1987* (eds Schmidt, S. C. and Holmes, N. C.), North-Holland, 1988, p. 703.
130. Car, R. and Parrinello, M., *Phys. Rev. Lett.*, 1985, **55**, 2471.
131. Galli, G., Martin, R. M., Car, R. and Parrinello, M., *Science*, 1990, **250**, 1547.
132. Taylor, P. A. and Dodson, W., in *Shock Compression of Condensed Matter—1989* (eds Schmidt, S. C., Johnson, J. N. and Davison, L. W.), Elsevier Science, 1990, p. 165.
133. Holian, B. L., *Phys. Rev.*, 1988, **A37**, 2562.
134. Vaidya, S. N. and Kennedy, G. C., *J. Phys. Chem. Solids*, 1970, **31**, 2329.
135. Ruoff, A. L., Xia, H., Luo, H. and Vohra, Y. K., *Rev. Sci. Instrum.*, 1990, **61**, 3830; also see Amato, I., *Sci. News*, Feb. 2, 1991, **139**, 72.
136. Van Thiel, M., *Compedium of Shock Wave Data*, Lawrence Livermore Laboratory Report UCRL 50108, 1977.
137. Mitchel, A. C. and Nellis, W. J., *J. Appl. Phys.*, 1981, **52**, 3363.
138. Trainor, R. J., Shaner, J. W., Auerbach, J. M. and Holmes, N. C., *Phys. Rev. Lett.*, 1979, **42**, 1154.
139. Vladimirov, A. S. *et al.*, *JETP Lett.*, 1984, **39**, 82.
140. Weingart, R. C., Lawrence Livermore Laboratory Report UCRL 52752, 1979.
141. Hawke, R. S. and Scudder, J. K., *High Pressure Science and Technology* (eds Vodar, B. and Marteau, Ph.), Pergamon, 1980, vol. 2, p. 979.
142. Hawke, R. S. *et al.*, *J. Appl. Phys.*, 1972, **43**, 2734.